JOC The Journal of Organic Chemistry

NOTE

pubs.acs.org/joc

Aromaticity and Activation Strain Analysis of [3 + 2] Cycloaddition Reactions between Group 14 Heteroallenes and Triple Bonds

Israel Fernández,*[,†] Fernando P. Cossío,*[,‡] and F. Matthias Bickelhaupt*[,§]

[†]Departamento de Química Orgánica, Facultad de Química, Universidad Complutense, 28040 Madrid, Spain

[‡]Departamento de Química Orgánica I-Kimika Organikoa I Saila, Facultad de Química-Kimika Fakultatea, Universidad del País Vasco-Euskal Herriko Unibertsitatea, P. K. 1072, 20080 San Sebastián-Donostia, Spain

[§]Department of Theoretical Chemistry and Amsterdam Center for Multiscale Modeling, Scheikundig Laboratorium der Vrije Universiteit, De Boelelaan 1083, 1081 HV Amsterdam, The Netherlands

Supporting Information

ABSTRACT: We have computationally explored the trend in reactivity of [3 + 2] cycloaddition reactions between $H_2E{=}C{=}PH$ and $HC{\equiv}CH$ as the terminal position in the phosphaallene is varied along E = C, Si, Ge, Sn, Pb. The reaction barrier drops significantly from E = C (nearly 50 kcal/mol) to E = Si−Pb (ca. 20 kcal/mol). Activation strain analyses tie this trend to a reduction in activation strain in the heavier phosphaallene analogues which, in contrast to the parent compound $H_2C{=}C{=}PH$, do already possess the bent geometry required in the TS.

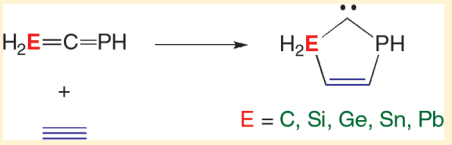

In recent years, allenes, and in particular electron-deficient allenes, have emerged as attractive building blocks in organic synthesis.[1] This growing interest is mainly due to the development of efficient methods for the preparation of allenes based on either classical organic chemistry or organometallic reagents.[2−4] In contrast, their heavier analogues E=C=E′ (E, E′ = Si, Ge, Sn, N, P, As) have received much less attention because they have been only postulated as transient intermediates for a long time. However, heavier heteroallenes, such as phosphaallenes P=C=X′ and $R_3P{=}C{=}PR_3$ or metallaallenes E=C=C (E = Si, Ge) can be successfully synthesized as stable or transient derivatives by using bulky substituents,[5−13] which kinetically stabilize the reactive double bonds.

Very recently, it has been reported that heteroallene **1** is readily converted into the tricyclic compound **2** when reacted with methyl acetylenedicarboxylate (Scheme 1).[14] With the help of DFT calculations, it has been proposed that a concerted [3 + 2] cycloaddition reaction occurs to initially produce the carbene intermediate **3**, which evolves to the isolated product **2**.

In our ongoing interest in the effect of introducing metal moieties in pericyclic reactions,[15−18] the experimentally observed transformation depicted in Scheme 1 prompted us to computationally study this novel [3 + 2] cycloaddition. Given the tremendous importance of [3 + 2] cycloadditions in organic chemistry,[19] we decided to carry out a comparative study on the effect of the group 14 elements in allenes **4a**−**f** ($H_2E{=}C{=}PH$, E = C−Pb) in their reaction toward triple bonds. Issues such as the in-plane aromaticity of the corresponding transition states shall be discussed. Furthermore, the origins of the reaction barriers will be studied by means of the so-called activation strain model.

First, we consider the reaction between allenes **4** and acetylene to produce the corresponding carbenes **5** (see Table 1). All

Scheme 1. [3 + 2] Cycloaddition Reaction of Heteroallene 1 with Methyl Acetylenedicarboxylate To Produce Compound 2

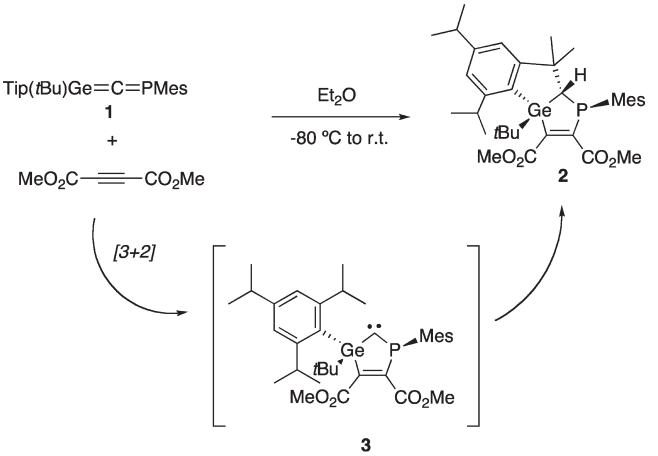

Tip = 2,4,6-triisopropylphenyl, Mes = 2,4,6-tri-*tert*-butylphenyl

processes occur via a concerted $[{}_{\pi}4_s + {}_{\pi}2_s]$ cycloaddition mechanism through quite symmetrical transition structures (see Figure 1). A single-point CASSCF(2,2)/6-31G*&LANL2DZ calculation on **TS3** in which the Ge atom was described with an effective core potential (ECP, vide infra) showed that the occupancies of the active CI space are 1.851 e and 0.149 e, thus indicating that the closed-shell configuration of this transition

Received: December 27, 2010
Published: March 09, 2011

 © 2011 American Chemical Society

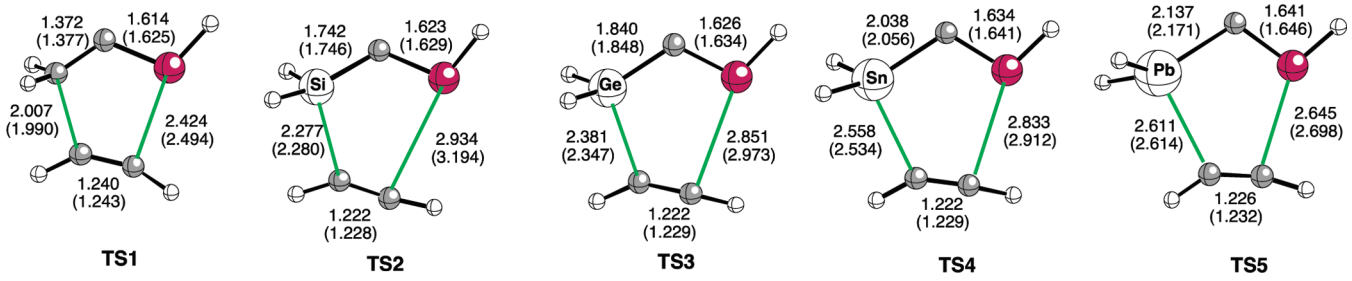

Figure 1. Geometries (in Å) of the transition states of our [3 + 2] cycloadditions, optimized at M06-2X/def-TZVPP (B3LYP/def2-TZVPP geometry parameters in parentheses). Atoms are represented as spheres: C, gray; H, white; P, violet.

Table 1. Computed Barrier Energies ($\Delta G^{\ddagger}_{298}$, in kcal/mol), Reaction Energies ($\Delta G_{R,298}$, in kcal/mol) and NICS(R_p) (in ppm) for the Reaction of Compounds 4 with Acetylene

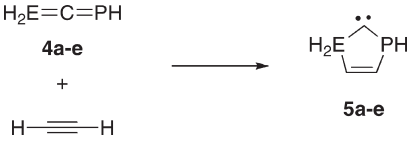

entry	E	$\Delta G^{\ddagger}_{298}$[a]	$\Delta G_{R,298}$[a]	$NICS(R_p)$[b]
a	C	47.3 (48.3)	11.6 (11.3)	−21.3
b	Si	20.1 (18.1)	−18.9 (−26.8)	−10.6
c	Ge	20.4 (17.9)	−14.5 (−23.8)	−12.4
d	Sn	18.4 (14.0)	−13.6 (−24.2)	−13.6
e	Pb	20.6 (15.4)	−5.0 (−14.2)	−14.7

[a] Plain values computed at the B3LYP/def2-TZVPP level. Values in parentheses were computed at the M06-2X/def2-TZVPP level. [b] Computed at the GIAO-B3LYP/def2-TZVPP level at the [3,+1] ring critical point (R_p) of the electron density.

structure accounts for ca. 93% of the CASSCF wave function. Therefore, in the remaining hybrid DFT calculations, only monodeterminantal electronic descriptions will be considered. Moreover, the negative nuclear independent chemical shift (NICS) values computed for our C_s-symmetric saddle points (Table 1) clearly suggest aromatic diatropic ring currents.[20] These NICS values were calculated at the [3,+1] ring critical point of the electron density, as defined in QTAIM,[21] due to its high sensitivity to diamagnetic effects and its unambiguous character to define the "center" of a ring in terms of electron density.

Similar to nonorganometallic [3 + 2] cycloaddtion reactions,[22,23] the six electrons involved in the concerted process lie approximately in the molecular plane and give rise to an appreciable ring current. In turn, this ring current promotes a strong diamagnetic shielding at the ring critical point, leading to the observed negative NICS values. The delocalization of the six electrons can be viewed with the help of the anisotropy of the induced current density (ACID) method, developed by Herges.[24,25] The in-plane aromaticity for **TS3** is clearly represented by the diamagnetic current along the toroid shown in Figure S2 of the Supporting Information. The in-plane aromatic character of **TS3** is nicely confirmed also by the expected "bell-shaped plot" of the NICS along the z axis perpendicular to the molecular plane, with a maximum NICS value at z = 0 Å: i.e., in the [3,+1] ring critical point (Figure 2).

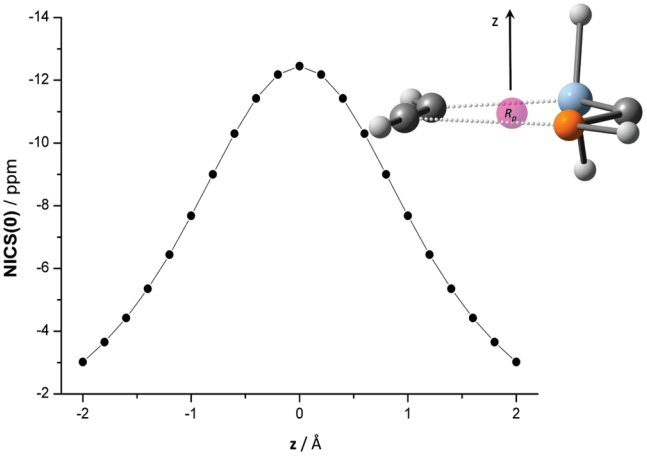

Figure 2. Plot of the computed NICS values along the z axis perpendicular to the molecular plane for **TS3**.

Interestingly, the computed energy values (Table 1) show that while the transformation involving the parent allene (H_2C=C=PH, **4a**) is endergonic, possessing a quite high activation barrier, the corresponding [3 + 2] cycloaddition reactions involving the heavier group 14 elements **4b**−**e** are highly exergonic, with activation barriers easily reached at room temperature. In view of the computed energies, it can be concluded that the presence of a group 14 element heavier than carbon in allenes **4** facilitates the cycloaddition process.

In order to understand the factors which control how the reaction barriers arise, we use the so-called activation strain analyses.[26−37] The activation strain model is a systematic extension of the fragment approach from equilibrium structures to transition states as well as nonstationary points: e.g., points along a reaction coordinate. It is a fragment approach to understanding chemical reactions, in which the height of reaction barriers is described and understood in terms of the original reactants. Thus, the potential energy surface $\Delta E(\zeta)$ is decomposed, along the reaction coordinate ζ, into the strain energy $\Delta E_{strain}(\zeta)$ associated with deforming the individual reactants plus the actual interaction energy $\Delta E_{int}(\zeta)$ between the deformed reactants:

$$\Delta E(\zeta) = \Delta E_{strain}(\zeta) + \Delta E_{int}(\zeta) \quad (1)$$

The strain term $\Delta E_{strain}(\zeta)$ is determined by the rigidity of the reactants and on the extent to which groups must reorganize in a particular reaction mechanism, whereas the interaction term $\Delta E_{int}(\zeta)$ between the reactants depends on their electronic structure and on how they are mutually oriented as they

dx.doi.org/10.1021/jo102572x |J. Org. Chem. 2011, 76, 2310–2314

approach each other. It is the interplay between $\Delta E_{strain}(\zeta)$ and $\Delta E_{int}(\zeta)$ that determines if and at which point along ζ a barrier arises. In the transition state (i.e., for $\zeta = \zeta_{TS}$), we arrive at the activation energy as a sum of activation strain plus TS interaction:

$$\Delta E^{\ddagger}(\zeta_{TS}) = \Delta E^{\ddagger}_{strain}(\zeta_{TS}) + \Delta E^{\ddagger}_{int}(\zeta_{TS}) \qquad (2)$$

Further details of the method can be found in the literature.[26−33]

In our activation strain diagrams, we have projected the intrinsic reaction coordinate (IRC) onto the $H_2E\cdots C(\equiv C)$ distance between the group 14 element of allenes **4a,c** and the carbon atom of the acetylene fragment. This reaction coordinate ζ undergoes a well-defined change in the course of the reaction from ∞ to the equilibrium E−C distance in the corresponding transition structure (Figure 3).

For the reaction of **4a** and acetylene we can see that, in the early stages of the process, the reaction profile ΔE raises monotonically as the reactants approach each other: i.e., there is no reactant-complex well. Interestingly, a sharp increase of ΔE occurs in the proximity of the transition-structure region, leading to the observed high reaction barriers. In contrast, the increase in ΔE in the **4c** + acetylene reaction is much less pronounced, in agreement with the much lower computed activation barrier.

Our activation strain analyses reveal that, for **4a** at long C···C distances, the interaction energy between the deformed reactants (ΔE_{int}) is at first destabilizing and thus contributes to the destabilization of the net energy ΔE, as can be seen in Figure 3a. The initial increase of ΔE_{int} can be traced to steric (Pauli) repulsion between the reactants in the early stages of the reaction. This behavior of ΔE_{int} is interesting, as it differs from reactions such as S_N2 substitution[26] and E2 elimination[33] but resembles the behavior in the pericyclic double group transfer reactions.[38,39] If we now further proceed along the reaction coordinate, ΔE_{int} inverts at a certain point, after which this term becomes more and more stabilized as one further approaches the transition state.

The situation is different for the reaction of **4c** with acetylene. Here the interaction does not at first become destabilizing. It remains practically unaltered at long Ge···C distances and then smoothly becomes stabilizing in the vicinity of the transition states (Figure 3b). As can be seen in Figure 3, the transition-state interaction term $\Delta E^{\ddagger}_{int}$ is about −10 kcal/mol in both **TS1** and **TS3**. The reason that **TS3** is associated with a lower overall barrier $\Delta E^{\ddagger}$ than **TS1** is the reduced activation strain energy $\Delta E^{\ddagger}_{strain}$ in the former. Thus, the activation strain constitutes the dominant factor controlling the relative barrier heights in our model reactions.

The sharp increase in ΔE_{strain} for the reaction between **4a** and acetylene comes mainly from the energy needed to deform the allene **4a** from its practically linear equilibrium geometry (C═C═P angle of 174.8°) to the bent geometry adopted in **TS1** (C═C═P angle of 120.8°; see Figure 1). The computed associated strain energy of this fragment is 29.6 kcal/mol. In contrast, the equilibrium geometry of **4c** is already more TS-like (Ge═C═P angles of 168.1 and 117.5° in **4c** and **TS3**, respectively). This fact can be rationalized considering the well-known reluctance of Si−Pb atoms to undergo s,p hybridization compared to carbon[40,41] which is, for instance, reflected in the remarkable geometric difference between linear acetylene C_2H_2 and the most stable (nonlinear) structures of its heavier E_2H_2 homologues.[42] Therefore, there is less need to deform heteroallene **4c**, which is translated into a much lower activation strain

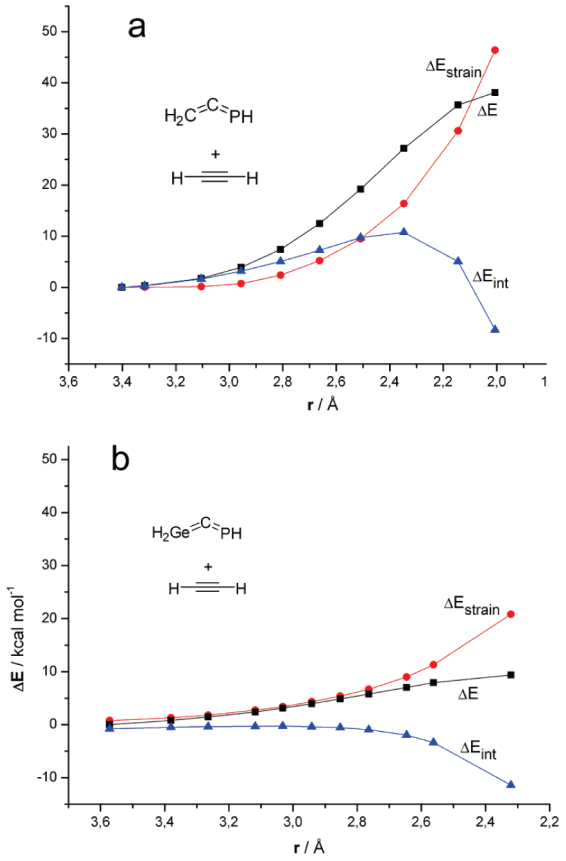

Figure 3. Activation strain analysis of the [3 + 2] cycloaddition reaction between acetylene and allene **4a** (a) and **4c** (b) along the reaction coordinate projected onto the E···C bond length (in Å). All data have been computed at the M06-2X/def2-TZVPP level.

(12.4 kcal/mol) and, therefore, into a much lower activation barrier. The deformation of the acetylene fragment in the transition state also contributes to the total activation strain, but it does so to a lesser extent (16.8 kcal/mol for the **4a** + acetylene reaction vs 8.4 kcal/mol for the **4c** + acetylene cycloaddition).

To further illustrate the activation-strain control of the process, we plotted the computed total activation barriers ($\Delta E_a = E(TS) - E(4) - E(acetylene)$) versus the total activation-strain energies $\Delta E^{\ddagger}_{strain}$ (computed as the sum of the individual strain energies of both reactants). Figure S1 of the Supporting Information clearly shows that both parameters are nicely linearly correlated (correlation coefficient of 0.9998 and standard deviation of 0.3 kcal/mol). This result confirms that the activation strain is decisive in determining the barrier heights of [3 + 2] cycloaddition reactions.[36] Our results also show that the high barrier for the [3 + 2] cycloaddition of **4a** occurs, despite the aromatic character of the corresponding TS, because of the need to deform this heteroallene from linearity to a bent geometry in the transition state.

In order to assess the generality of these results, we extended our study to the more realistic system reported in Figure 4: namely, the reaction between germallene **1b** and dimethyl acetylenedicarboxylate to yield intermediate carbene **3b** and, after the corresponding insertion reaction, tricyclic compound **2b**. This model reaction includes all the relevant features of the systems reported by Ghereg et al.[14] (Scheme 1). At the relatively

dx.doi.org/10.1021/jo102572x |J. Org. Chem. 2011, 76, 2310–2314

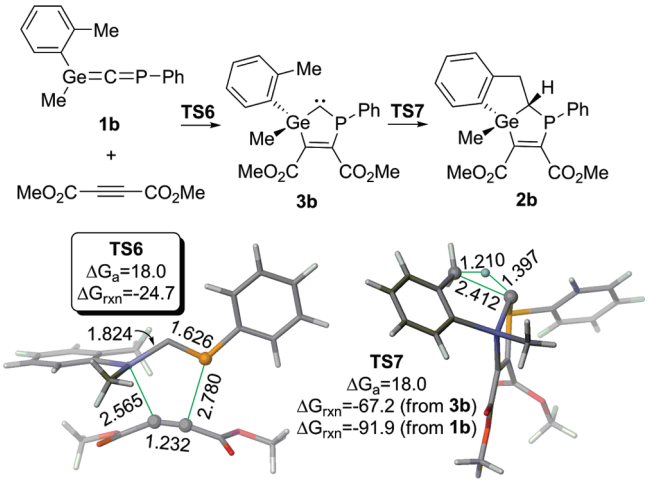

Figure 4. Main geometric (in Å) and energetic features (in kcal/mol) of the reaction between germallene **1b** and dimethyl acetylenedicarboxylate, computed at the M06-2X/6-31G*&LANL2DZ level.

less demanding M06-2X/6-31G&LANL2DZ level of theory, with an ECP for Ge, the activation free energy associated with the formation of **3b** via **TS6** is similar to that computed for **TS3** at a higher computational level (Table 1). Similarly, densely substituted carbene **3b** is more stable than the reactants, the corresponding Gibbs reaction energy being in line with the value obtained for the parent reaction with E = Ge (Table 1). The computations show that the insertion reaction requires an activation free energy similar to that obtained for the [3 + 2] step (Figure 4), the corresponding transition structure **TS7** being quite synchronous. The overall reaction is computed to be very exothermic, thus providing a considerable thermodynamic driving force for the whole process.

In conclusion, our [3 + 2] cycloaddition reactions between heteroallenes $H_2E{=}C{=}PH$ (E = C−Si; **4a**−**e**) and acetylene occur concertedly through C_s-symmetric and in-plane aromatic transition states. Reaction barriers drop significantly if one goes from E = carbon to the heteroallenes with heavier group 14 elements E. Our activation strain analyses identify the activation strain as the major factor in controlling the barrier heights. The activation strain is high in the case of $H_2C{=}C{=}PH$, causing the barrier to be high as well, despite the aromatic character of the TS. The reason is that this heteroallene **4a** is linear and must be bent significantly in the TS. At variance with this, the heteroallenes with a heavier group 14 element E do already possess a bent equilibrium geometry which better fits into the TS structure and therefore requires less deformation. The conclusions obtained for these simple model reactions can be extended to the densely substituted systems used in experimental studies.

COMPUTATIONAL DETAILS

All of the calculations reported in this paper were obtained with the GAUSSIAN 09 suite of programs.[43] All reactants, transition states, and cycloadducts were optimized using the hybrid functional B3LYP[44,45] and Truhlar's meta hybrid exchange-correlation functional M06-2X[46] with the triple-ζ-quality def2-TZVPP basis sets,[47] which are supposed to be close to the DFT basis set limit. In order to assess the reliability of less demanding basis sets, the split-valence 6-31G* and LANL2DZ ECP (for Ge) basis sets were also tested.[48] Reactants and products were characterized by frequency calculations and have positive definite Hessian matrices. Transition structures (TS's) show only one negative eigenvalue in their diagonalized force constant matrices, and their associated eigenvectors were confirmed to correspond to the motion along the reaction coordinate under consideration using the intrinsic reaction coordinate (IRC) method.[49] NICS values have been computed using the gauge invariant atomic orbital (GIAO) method[50] at the GIAO-B3LYP/def2-TZVPP level, since this method is more useful for comparative purposes.[20]

ASSOCIATED CONTENT

Supporting Information. Text, tables, and figures giving Cartesian coordinates (in Å) and total energies (in au, noncorrected zero-point vibrational energies included) of all the stationary points discussed in the text, the complete ref 43, and Figures 1S and 2S. This material is available free of charge via the Internet at http://pubs.acs.org.

AUTHOR INFORMATION

Corresponding Author

*E-mail: israel@quim.ucm.es; fp.cossio@ehu.es; f.m.bickelhaupt@vu.nl.

ACKNOWLEDGMENT

We are grateful for financial support from the Spanish MICINN and CAM (Grants CTQ2010-20714-C02-01, CTQ2010-16959 Consolider-Ingenio 2010, CSD2007-00006, S2009/PPQ-1634, and Ramón y Cajal contract to I.F.) and The Netherlands Organization for Scientific Research (NWO-CW).

REFERENCES

(1) Ma, S. *Chem. Rev.* **2005**, *105*, 2829.
(2) Miesch, M. *Synthesis* **2004**, 746.
(3) Hoffmann-Röder, A.; Krause, N. *Angew. Chem., Int. Ed.* **2002**, *41*, 2933.
(4) Krause, N.; Hoffmann-Röder, A. *Tetrahedron* **2004**, *60*, 11671.
(5) Escudié, J.; Ranaivonjatovo, H.; Rigon, L. *Chem. Rev.* **2000**, *100*, 3639.
(6) Eichler, B.; West, R. *Adv. Organomet. Chem.* **2001**, *46*, 1.
(7) Escudié, J.; Ranaivonjatovo, H. *Organometallics* **2007**, *26*, 1542.
(8) Appel, R. In *Multiple Bonds and Low Coordination in Phosphorus Chemistry*; Regitz, M., Scherer, O. J., Eds.; Thieme: Stuttgart, Germany, 1990; pp 157−219.
(9) Yoshifuji, M. *Dalton Trans.* **1998**, 3343.
(10) Rigon, L.; Ranaivonjatovo, H.; Escudié, J.; Dubourg, A.; Declercq, J.-P. *Chem. Eur. J.* **1999**, *5*, 774.
(11) Transient $R^1R^2Ge{=}C{=}PR_3$: Ramdane, H.; Ranaivonjatovo, H.; Escudié, J.; Mathieu, S.; Knouzi, N. *Organometallics* **1996**, *15*, 3070.
(12) Stable $R^1R^2Ge{=}C{=}PR_3$: El Harouch, Y.; Gornitzka, H.; Ranaivonjatovo, H.; Escudié, J. *J. Organomet. Chem.* **2002**, *643*−*644*, 202.
(13) Transient $R_3P{=}C{=}PR_3$: Marrot, S.; Kato, T.; Cossío, F. P.; Gornitzka, H.; Baceiredo, A. *Angew. Chem., Int. Ed.* **2006**, *45*, 7447.
(14) Ghereg, D.; André, E.; Sotiropoulos, J.-M.; Miqueu, K.; Gornitzka, H.; Escudié, J. *Angew. Chem., Int. Ed.* **2010**, *49*, 8704.
(15) Fernández, I.; Sierra, M. A.; Cossío, F. P. *J. Org. Chem.* **2006**, *71*, 6178.
(16) Fernández, I.; Cossío, F. P.; Sierra, M. A. *Organometallics* **2007**, *26*, 3010.
(17) Fernández, I.; Sierra, M. A.; Cossío, F. P. *J. Org. Chem.* **2008**, *73*, 2083.

(18) Fernández, I.; Cossío, F. P.; de Cózar, A.; Lledós, A.; Mascareñas, J. L. *Chem. Eur. J.* **2010**, *16*, 12147.
(19) *Synthetic Applications of 1,3-Dipolar Cycloaddition Chemistry Toward Heterocycles and Natural Products*; Padwa, A., Pearson, W. H., Eds.; Wiley: New York, 2002.
(20) Chen, Z.; Wannere, C. S.; Corminboeuf, C.; Puchta, R.; Schleyer, P. v. R. *Chem. Rev.* **2005**, *105*, 3842.
(21) Bader, R. F. W. *Atoms in Molecules: A Quantum Theory*; Clarendon: Oxford, U.K., 1990.
(22) Morao, I.; Lecea, B.; Cossío, F. P. *J. Org. Chem.* **1997**, *62*, 7033.
(23) Cossío, F. P.; Morao, I.; Jiao, H.; Schleyer, P. v. R. *J. Am. Chem. Soc.* **1999**, *121*, 673.
(24) Herges, R.; Geuenich, D. *J. Phys. Chem. A* **2001**, *105*, 3214.
(25) Geuenich, D.; Hess, K.; Köhler, F.; Herges, R. *Chem. Rev.* **2005**, *105*, 3758.
(26) Bickelhaupt, F. M. *J. Comput. Chem.* **1999**, *20*, 114.
(27) Diefenbach, A.; Bickelhaupt, F. M. *J. Chem. Phys.* **2001**, *115*, 4030.
(28) Diefenbach, A.; Bickelhaupt, F. M. *J. Phys. Chem. A* **2004**, *108*, 8460.
(29) Diefenbach, A.; de Jong, G. T.; Bickelhaupt, F. M. *J. Chem. Theory Comput.* **2005**, *1*, 286.
(30) van Stralen, J. N. P.; Bickelhaupt, F. M. *Organometallics* **2006**, *25*, 4260.
(31) de Jong, G. T.; Bickelhaupt, F. M. *ChemPhysChem* **2007**, *8*, 1170.
(32) de Jong, G. T.; Bickelhaupt, F. M. *J. Chem. Theory Comput* **2007**, *3*, 514.
(33) Bento, A. P.; Bickelhaupt, F. M. *J. Org. Chem.* **2008**, *73*, 7290.
(34) Fernández, I.; Frenking, G.; Uggerud, E. *Chem. Eur. J.* **2009**, *15*, 2166.
(35) Fernández, I.; Frenking, G.; Uggerud, E. *J. Org. Chem.* **2010**, *75*, 2971.
(36) Ess, D. H.; Houk, K. N. *J. Am. Chem. Soc.* **2008**, *130*, 10187.
(37) Legault, C. Y.; Garcia, Y.; Merlic, C. A.; Houk, K. N. *J. Am. Chem. Soc.* **2007**, *129*, 12664.
(38) Fernández, I.; Bickelhaupt, F. M.; Cossío, F. P. *Chem. Eur. J.* **2009**, *15*, 13022.
(39) Fernández, I.; Cossío, F. P. *Curr. Org. Chem.* **2010**, *14*, 1578.
(40) Kutzelnigg, W. *Angew. Chem., Int. Ed.* **1984**, *23*, 272.
(41) Kaupp, M.; Schleyer, P. v. R. *J. Am. Chem. Soc.* **1993**, *115*, 1061.
(42) Lein, M.; Krapp, A.; Frenking, G. *J. Am. Chem. Soc.* **2005**, *127*, 6290.
(43) Frisch, M. J. et al. *Gaussian 09, Revision B.1*; Gaussian, Inc., Wallingford, CT, 2009.
(44) Becke, A. D. *J. Chem. Phys.* **1993**, *98*, 5648.
(45) Lee, C.; Yang, W.; Parr, R. G. *Phys. Rev. B* **1998**, *37*, 785.
(46) Zhao, Y.; Truhlar, D. G. *Acc. Chem. Res.* **2008**, *41*, 157.
(47) Weigend, F.; Alhrichs, R. *Phys. Chem. Chem. Phys.* **2005**, *7*, 3297.
(48) Hay, P. J.; Wadt, W. R. *J. Chem. Phys.* **1985**, *82*, 299.
(49) González, C.; Schlegel, H. B. *J. Phys. Chem.* **1990**, *94*, 5523.
(50) Wolinski, K.; Hinton, J. F.; Pulay, P. *J. Am. Chem. Soc.* **1990**, *112*, 8251.